ELECTRON CRYSTALLOGRAPHIC STUDY OF INCOMMENSURATE MODULATION IN THE Pb-DOPED Bi-2223 HIGH Tc SUPERCONDUCTING PHASE *

Y.D. Mo[†], T.Z. Cheng[‡], H.F. Fan[†, ‡, **], J.Q. Li[§], B.D. Sha[‡], C.D. Zheng[†], F.H. Li[†] & Z.X. Zhao[†, §]

† *Institute of Physics, Chinese Academy of Sciences, Beijing 100080, China.*
‡ *Lab. of Structure Research, Univ. of Science and Technology of China, Hefei 230026, China.*
§ *National Laboratory for Superconductivity, Chinese Academy of Sciences, Beijing 100080, China.*

Incommensurate modulation is a common feature of the Bi-cuprate superconductors. However there have been very few reports on structural investigation of the Pb-doped Bi-2223 phase, since it is very difficult to prepare suitable single crystals for X-ray diffraction analysis. Furthermore the methods commonly used for solving incommensurate modulated structures are "trial and error" ones, they are not suitable in complicated cases such as that of the Pb-doped Bi-2223 phase. In our work, electron diffraction was used instead of X-ray diffraction. This facilitates the investigation of micro-crystalline samples and the observation of oxygen atoms in the presence of much heavier atoms such as bismuth. The multi-dimensional direct method was used for the diffraction analysis. With this method there is no need to assume any modulation model before the modulation waves are measured directly on the potential distribution function derived from the experimental data. The result shows that the structure contains simultaneously occupational and positional modulation and the layers Cu(2)-Ca-Cu(1)-Ca-Cu(2) are bridged by disordered oxygen atoms.

---

* Supported in part by the national natural science foundation of China
and by the united nations educational, scientific and cultural organization

** To whom correspondences should be addressed

1. INTRODUCTION

Pb-doped Bi-2223 phase is the highest Tc phase in the Bi-Sr-Ca-Cu-O system. Ikeda, Aota, Hatano & Ogawa[1] obtained high resolution electronmicrographs of the Pb-doped Bi-2223 phase. Incommensurate modulation was observed but very limited structural details have been recognized. The electron diffraction study by Li, Yang, Li, Zhou, Zheng, Ni, Jia & Zhao[2] gave the super-space group and the corresponding unit cell parameters but no further details on the modulation. Sequeira, Yakhmi, Iyer, Rajagopal & Sastry[3] reported the analysis using neutron powder diffraction technique, from which only the average structure have been determined. There remains great interest on the incommensurate modulation of the Pb-doped Bi-2223 phase. The purpose of the present work is to find the structural details of the incommensurate modulation. Our approach is electron diffraction analysis with the multi-dimensional direct methods newly developed in our laboratories. The analysis is based on the symmetry and unit cell parameters found by Li *et al.*[2] and the average structure obtained by Sequeira *et al.*[3].

2. EXPERIMENT

Specimens with the nominal composition of $Bi_{1.6}Pb_{0.4}Sr_2Ca_2Cu_3O_y$, after grinding and ion thinning, were used for taking electron micrographs. A Hitachi H-9000 electron microscope was used to carry out electron diffraction experiment. One-dimensional modulation parallel to the **b** axis is clearly seen on the electron diffraction pattern normal to the **a** axis. The super-space group has been determined by Li *et al.*[2] as P:Bbmb:1-11. The main and satellite reflections can be indexed as *0klm* using a four-dimensional reciprocal lattice, the lattice vector of which is expressed as

$$\mathbf{H} = h\mathbf{a}^* + k\mathbf{b}^* + l\mathbf{c}^* + m\mathbf{q} \quad ,$$

where **a***, **b*** and **c*** define a reciprocal unit cell which corresponds to the three-dimensional unit cell in real space with parameters a=5.49Å, b=5.41Å, c=37.1Å, $\alpha=\beta=\gamma=90^o$. **q** (=0.117**b***) is the modulation wave vector. The modulation wave is thus parallel to the **b** axis with a period of 46.2Å, 8.54 times longer than b. Five photographs were taken with different exposure times for the same electron diffraction pattern. This is an analog of the multi-film method in X-ray crystallography for the collection of diffraction intensities. A Perkin Elmer PDS microdensitometer data acquisition system with a 20×20 μm^2 aperture was used to digitize the photographs. The whole pattern was divided into 2251×2251 pixels. The integrated intensity of each reflection was obtained by summing up the density, $\ln(I_o/I)$, of the pixels within the diffraction spot and then subtracting the background. Diffraction intensities were finally calibrated with the exposure time. Structure factor amplitudes were obtained as the square root of diffraction intensities. The R-factor for the discrepancy among symmetrically related reflections is 0.12 for the main and 0.13 for the satellite reflections. There are in total 112 independent *0klm* observed reflections including 42 main and 70 first-order satellite reflections. A few second-

order satellites were also observed, however they are much weaker than the first-order ones and hence are treated as unobserved reflections.

3. DIRECT PHASING OF THE SATELLITE REFLECTIONS

The structure analysis was carried out in four-dimensional space, in which the real and reciprocal unit cells are defined respectively by

$$\mathbf{a}_1 = \mathbf{a},\ \mathbf{a}_2 = \mathbf{b} - 0.117\mathbf{d},\ \mathbf{a}_3 = \mathbf{c},\ \mathbf{a}_4 = \mathbf{d}$$

and

$$\mathbf{b}_1 = \mathbf{a}^*,\ \mathbf{b}_2 = \mathbf{b}^*,\ \mathbf{b}_3 = \mathbf{c}^*,\ \mathbf{b}_4 = 0.117\mathbf{b}^* + \mathbf{d},$$

where **d** is the unit vector normal to the three-dimensional space, i.e. a unit vector simultaneously perpendicular to the vectors **a**, **b**, **c**, **a***, **b*** and **c***. For details of the multidimensional representation of incommensurate modulated structures the reader is referred to the papers by de Wolff[4], de Wolff, Janssen, & Janner[5] and Yamamoto[6]. Phase derivation for the satellite reflections was based on the modified Sayre equation given by Hao, Liu & Fan[7]:

$$\mathbf{F}_s(\mathbf{H}) = 2\,(\theta/V)\Sigma_{\mathbf{H}'}\,[\mathbf{F}_m(\mathbf{H}')\,\mathbf{F}_s(\mathbf{H}-\mathbf{H}')] \quad , \qquad (1)$$

where **H** is a reciprocal lattice vector in four-dimensional space, $\mathbf{F}_s(\mathbf{H})$ denotes the structure factor for the satellite reflections, $\mathbf{F}_m(\mathbf{H})$ denotes that for the main reflections, θ is an atomic form factor; V is the volume of the three-dimensional unit cell of the average structure. According to (1) the phases of $\mathbf{F}_s(\mathbf{H})$ can be derived by a simple phase extension technique provided the phases of $\mathbf{F}_m(\mathbf{H})$ are known in advance. In the present work, a multi-solution random-starting phase extension procedure similar to that of Yao[8] was used. The starting set consists of 42 main reflections with known phases and 40 satellite reflections with random assigned phases. During the phase extension and refinement, the known phases were kept fixed. Resulting phase sets were evaluated by a residual figure of merit similar to that used in MULTAN[9], but with the normalized structure factors of X-ray diffraction replaced by the ordinary structure factors of electron diffraction:

$$R_\alpha = \Sigma_H\ |\alpha_{est} - \alpha| \,/\, \Sigma_H\,\alpha \quad , \qquad (2)$$

where

$$\alpha_{est} \sim \Sigma\,[\chi\, I_1(\chi) \,/\, I_2(\chi)\,] \quad ,$$

$$\alpha^2 = [\,\Sigma_{H'} \chi \sin\phi\,]^2 + [\,\Sigma_{H'} \chi \cos\phi\,]^2 \quad ,$$

$$\chi = 2\sigma_3\sigma_2^{-3/2} \,|\, \mathbf{F(H)F(H')F(H\text{-}H')} \,| \quad ,$$

$$\phi = \varphi_{H'} + \varphi_{H-H'} \quad .$$

The residual figure of merit R_α is equivalent to the R_{Karle} figure of merit defined by Karle & Karle[10]. For comparing the effects of different known-phase sets of the main reflections on the resulting phases of the satellites, three different known-phase sets were used separately as the fixed part of the starting set. The first known-phase set was calculated from the average structure, the second set was calculated using only the metal atoms of the average structure, while the phases of the third set were just randomly assigned to be 0 or π. 100 random trials were calculated for each known-phase set. Among the 100 trials based on the first known-phase set, the residual figures of merit ranges from 0.33 to 0.67. The resulting phase set corresponding to the minimum residual figure of merit was selected to calculate the Fourier map $\varepsilon_0 \int_0^1 \varphi(x_1, x_2, x_3, x_4)\,dx_1$, where $\varphi(x_1, x_2, x_3, x_4)$ is the potential distribution function of the structure in four-dimensional space and is a four-dimensional periodic function. x_1, x_2, x_3 and x_4 are fractional coordinates in the directions of $\mathbf{a}_1$, $\mathbf{a}_2$, $\mathbf{a}_3$ and $\mathbf{a}_4$ respectively. A section of the above Fourier map perpendicular to the $\mathbf{a}_4$ axis, i.e. the potential distribution function in three-dimensional space projected along the $\mathbf{a}_1$ axis, $\varphi(y,z)$, is shown in Fig. 1.

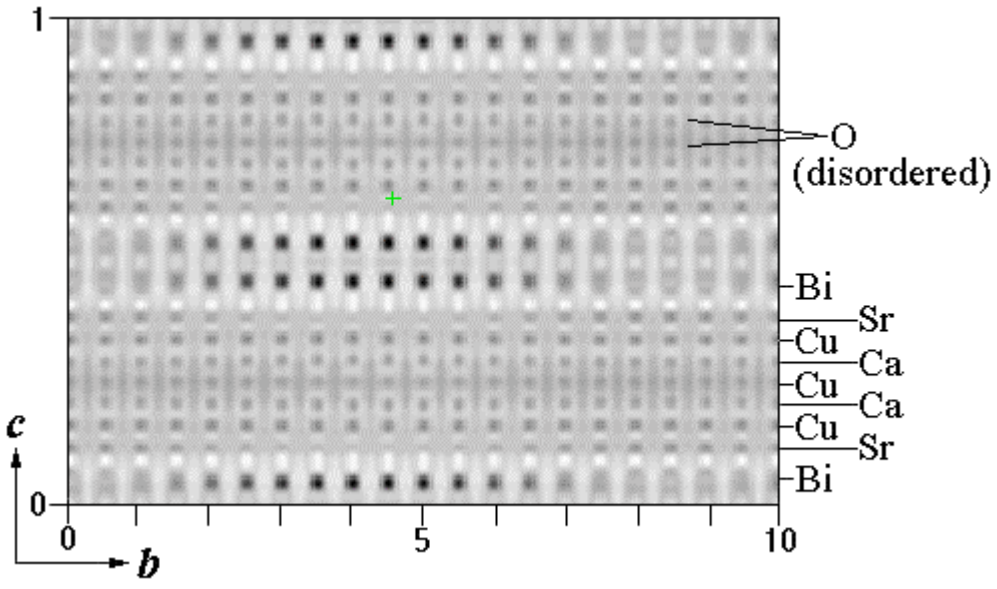

Fig. 1. $\varphi(y,z)$, three-dimensional potential distribution projected along the **a** axis, calculated with the direct-method phases (ten unit cells are plotted along the **b** axis).

Similarly, two Fourier maps were obtained based on the second and the third known-phase sets respectively. As is expected, the main features of the second Fourier map is similar to that of the first, while the third Fourier map is full of spurious peaks and is uninterpreted. This confirms that the direct-method results are reliable provided that the average structure used to calculate the phases of the main reflections is essentially correct. In Fig. 1 modulation on position and/or occupation is clearly observed for most of the atoms giving much more structural details in comparison of the high resolution electron micrographs obtained for the Pb-doped Bi-2223 phase.

4. FOURIER RECYCLING

Modulation waves were measured directly from $\varepsilon_0 \int_0^1 \varphi(x_1, x_2, x_3, x_4)\,dx_1$ for all except two oxygen atoms, which overlap with the Bi and Sr atoms respectively on the projection along the $\mathbf{a}_1$ axis. Modulation parameters were obtained by the Fourier series expansion of the resulting curves. Based on the modulation parameters of the metal atoms and parameters of the average structure, iterative Fourier calculation was carried out. All parameters except the temperature factors were adjusted after each cycle. The *R*-factor for the discrepancy between calculated and observed structure factors decreased from 0.55 to 0.32 for the main reflections and from 0.37 to 0.32 for the satellite reflections.

5. LEAST-SQUARES REFINEMENT

The total number of reflections used in the refinement is 182 including 42 observed main reflections, 70 first-order observed satellite reflections and 70 second-order unobserved satellite reflections with their structure factor magnitudes assigned to zero. Since the number of reflections is not enough for a full-matrix least-squares refinement, only part of the parameters were allowed to change within a single cycle. A few cycles of refinement led to an *R*-factor of 0.27 for the main and 0.22 for the first-order satellite reflections. The O(1) and O(2) atoms were separated respectively from overlapping with the Bi and Sr atoms during the least-squares refinement. At this stage it was found that there are two reflections (0400) and (0420) with abnormally large discrepancy between the observed and calculated magnitudes of the structure factor. This can be explained by the secondary diffraction effect, since there is a strong reflection (0020) which forms a three-phase structure invariant with (0400) and (0420). The last two reflections are then eliminated in the further refinement. Meanwhile, the Fourier map at this stage showed spread region of potential distribution at y = 0.25 and from z ~ 0.15 to 0.25. The region covers the expected oxygen sites on the Cu-O layers. Six oxygen atoms were introduced to fit the distribution by least-square refinement of their position and occupancy and by adjustment of their anisotropic temperature factors. The *R*-factor dropped from 0.27 to 0.22 for the main reflections by eliminating the two reflections (0400) and (0420). It further decreased to 0.15 for the main and 0.17 for the first-order satellite reflections by fitting the spread region of potential distribution with disordered oxygen atoms. The final *R*-factor calculated for all observed structure factors, including (0400) and (0420), is 0.22 for the main and 0.17 for the satellite reflections. The variation of the *R*-factor in various stages is summarized in Table 1. Atomic parameters are listed in Table 2. The final Fourier map $\varphi(y,z)$ is shown in Fig. 2. Abnormally large standard deviations can be seen in Table 2b. This is due to the lack of sufficient number of reflections for the least-squares refinement.

However, the reliability of the result is proved by the high quality of the final Fourier map together with the reasonable value of final R-factors.

TABLE 1

R-factor in Various Stages

Stage	R_m	R_s
Fourier iteration	0.32	0.32
Preliminary least squares refinement	0.27	0.22
Eliminating (0400) and (0420)	0.22	0.22
Fitting with disordered O-atoms	0.15	0.17
Including (0400) and (0420)	0.22	0.17

$R = \Sigma||F_O|-|F_C|| \,/\, \Sigma|F_O|$

R_m --- *R*-factor for the main reflections

R_s --- *R*-factor for the first-order satellite reflections

TABLE 2

(a) Atomic Parameters of the Average Structure of Pb-doped Bi-2223 Phase

Atom	x	y	z	P	B_{iso}	β_{22}	β_{33}
Bi	0.75	0.00	0.0528(3)	0.65(2)	1.0		
Sr	0.25	0.00	0.1201(4)	0.71(3)	1.0		
Cu(2)	0.75	0.00	0.1583(4)	0.93(4)	1.0		
Ca	0.25	0.00	0.1969(8)	0.51(3)	1.0		
Cu(1)	0.75	0.00	0.2500	0.96(5)	1.0		
O(1)	0.25	0.00	0.0408(31)	0.97(8)	1.0		
O(2)	0.75	0.00	0.1171(16)	0.96(8)	1.0		
O(3)	0.00	0.25	0.1568(10)	1.00(7)		0.00045	0.00010
O(4)	0.00	0.25	0.1810(10)	0.76(7)		0.00045	0.00010
O(5)	0.50	0.25	0.1863(7)	1.16(7)		0.00045	0.00010
O(6)	0.00	0.25	0.2122(9)	0.93(7)		0.00045	0.00010
O(7)	0.50	0.25	0.2146(8)	0.52(7)		0.00045	0.00010
O(8)	0.00	0.25	0.2470(40)	0.45(5)		0.00045	0.00010

The x coordinates are according to Sequeira *et al.*[3]

P --- occupancy ; $\beta_{22} = u_{22}b^{*2}$; $\beta_{33} = u_{33}c^{*2}$

(b) Modulation parameters of Pb-doped Bi-2223 phase

Atom	W_1	W_2	P_1	P_2
Bi	0.0038(2)	0.0006(2)	-0.267(12)	0.059(13)
Sr	-0.0006(3)	0.0002(2)	-0.043(11)	0.008(15)
Cu(2)	0.0007(2)	0.0001(2)	-0.064(21)	-0.001(19)
Ca	0.0017(5)	0.0007(5)	-0.172(30)	0.008(33)
Cu(1)	0.000.00	0.003(22)	0.001(25)	
O(1)	0.0085(9)	0.0038(7)	-0.293(61)	-0.207(55)
O(2)	-0.0008(11)	-0.0003(8)	0.342(53)	-0.024(43)
O(3)	0.0002(5)		0.014(36)	
O(4)	0.0009(6)		-0.056(47)	
O(5)	-0.0008(5)		0.005(38)	
O(6)	-0.0007(8)		0.025(30)	
O(7)	0.0006(4)		-0.122(64)	
O(8)	0.0020(26)		-0.092(63)	

$$U_z = 2W_1\cos 2\pi x_4 + 2W_2\cos 4\pi x_4; \quad P = 1 + 2P_1\cos 2\pi x_4 + 2P_2\cos 4\pi x_4$$

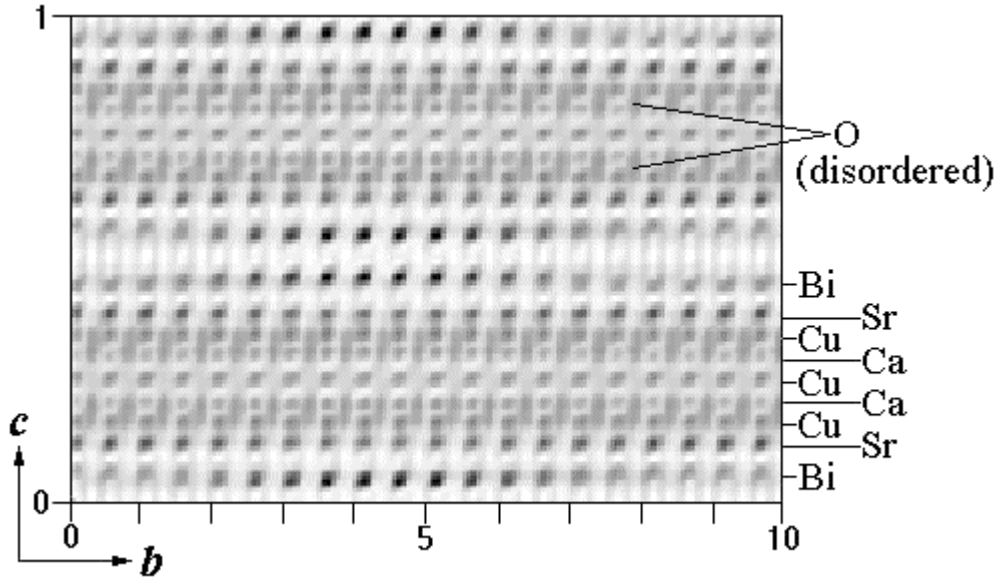

Fig. 2. $\varphi(y,z)$, three-dimensional potential distribution projected along the **a** axis, calculated with the phases after least-squares refinement (ten unit cells are plotted along the **b** axis).

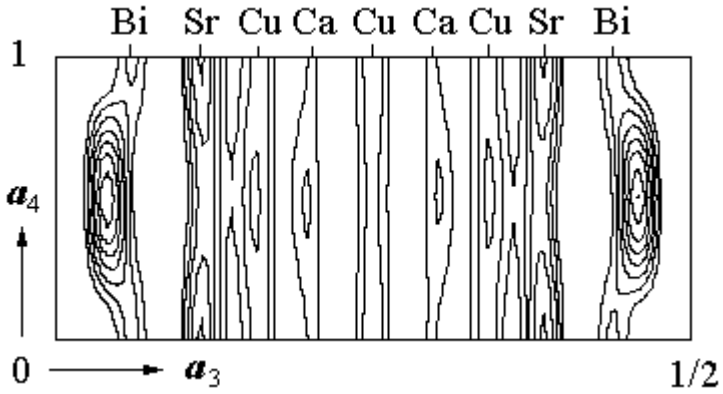

Fig. 3. $\int_0^1 \varphi(x_1, 0, x_3, x_4)dx_1$, a section-projection of the four-dimensional potential distribution.

6. DISCUSSION

A section of the final Fourier map $\int_0^1 \varphi(x_1, 0, x_3, x_4)dx_1$ at x_2 = 0 is shown in Fig. 3. An atom in the four-dimensional space without modulation will have a shape of an infinite straight rod parallel to the fourth dimension $\mathbf{a}_4$. Occupational modulation will periodically change the width, while positional modulation will periodically change the direction of the rod. It is seen that the potential at the sites of all metal atoms varies evidently along the $\mathbf{a}_4$ direction. This concludes that occupational modulation exists for all metal atoms. Besides, the coordinate x_4 for the maximum potential of all metal atoms except Cu(1) also varies with x_4 indicating the existence of positional modulation for all but Cu(1) metal atoms. The maximum displacement perpendicular to the $\mathbf{a}_1$ axis is about 0.31Å for Bi, 0.07Å for Sr, 0.04Å for Cu(2), 0.17Å for Ca and 0.00Å for Cu(1). On the other hand from the Fourier map, $\varphi(y,z)$, shown in Fig. 2, we can see how the atoms are modulated from one unit cell to the other. Both occupational and positional modulations are evident for Bi atoms. The strong occupational modulation of Bi atoms implies large amount of Bi-vacancies disordered on the planes normal to the **b** axis. This explains the low average occupancy (0.66) for Bi atoms. The same feature is also found for Ca and Sr atoms. Another prominent feature can be seen in Fig. 2 is that oxygen atoms of the Cu(1)-O layers move towards the Ca layer forming a disordered oxygen bridge across the layers of Cu(2)-Ca-Cu(1)-Ca-Cu(2). This implies the existence of large amount of O-vacancies on the Cu(1)-O layer. In addition, occupational and positional modulations along the **b** axis are also found for the disordered oxygen atoms.

It is seen that multi-dimensional direct methods are powerful for the determination of incommensurate modulated structures without relying on any hypothetical modulation model. The use of electron diffraction instead of X-ray or neutron diffraction is proved successful for the crystal structure analysis of micro-crystalline samples and for locating oxygen atoms in the presence of heavy metal atoms.

HFF is pleased to acknowledge the generous assistance of the Royal Society of London without whose support this work could not have been completed.

REFERENCES

[1] S. Ikeda, K. Aota, T. Hatano, & K. Ogawa, *Jpn. J. Appl. Phys*., **27** (1988), L2040.

[2] J.Q. Li, D.Y. Yang,, F.H. Li, P. Zhou, D.N. Zheng, Y.M. Ni, S.L. Jia, & Z.X. Zhao, *Progress in High Tc Superconductivity*, **22** (1989), 441.

[3] A. Sequeira, J.V. Yakhmi, R.M. Iyer, H. Rajagopal, & P.V.P.S.S.Sastry, *Physica C*, **167** (1990), 291.

[4] P.M. de Wolff, *Acta Cryst.*, A**30** (1974), 777.

[5] P.M. de Wolff, T. Janssen & A. Janner, *Acta Cryst*., A**37** (1981), 625.

[6] A. Yamamoto, *Acta Cryst.*, A**38** (1982), 87.

[7] Q. Hao, Y.W. Liu, & H.F. Fan, *Acta Cryst*., A**43** (1987), 820.

[8] J. X. Yao, *Acta Cryst*., A**39** (1983), 35.

[9] P. Main, S.J. Fiske, S.E. Hull, L. Lessinger, G. Germain, J.P. Declercq & M.M. Woolfson, *MULTAN8O: a system of computer programs for the automatic solution of crystal structures from X-ray diffraction data* (Univs. of York, England and Louvain, Belgium, 1980).

[10] J. Karle & I.L. Karle, *Acta Cryst.*, **21** (1966), 849.